

1 **Title: Common causes drive negative correlations between nuclear genetic**
2 **and species level biodiversity**

3 **Authors:** Chloé Schmidt^{1*}, Stéphane Dray², Colin J. Garroway^{1*}

4 **Affiliations:**

5 ¹Department of Biological Sciences, University of Manitoba, Winnipeg, Canada

6 ²Univ Lyon, Université Claude Bernard Lyon 1, CNRS, Laboratoire de Biométrie et Biologie
7 Evolutive, F-69100, Villeurbanne, France

8 *Correspondence to: schmid46@myumanitoba.ca, colin.garroway@umanitoba.ca

9 **Abstract:** We do not yet have a solid empirical understanding of the processes that produce
10 biogeographic patterns of species richness. This is partly due to a lack of knowledge about
11 corresponding spatial patterns of genome-wide diversity, which will be inextricably linked to
12 species richness. We use estimates of gene diversity calculated from open data to show that
13 genetic diversity and species richness share spatial structure. Species richness hotspots tend to
14 harbor low levels of within species genetic variation. Fitting multiple response and predictor
15 variables structured as a hypothesis network showed that a single model encompassing eco-
16 evolutionary processes related to environmental energy availability, niche availability, and
17 proximity to humans explains 75% of variation in the gene diversity gradient and 90% of the
18 variation in species-level diversity. This advances our understanding of the patterns and joint
19 causes of variation in the two most fundamental products of evolution.

20 **Keywords:** more individuals hypothesis, heterogeneity, latitudinal diversity gradient, carrying
21 capacity, Anthropocene, macroecology, macroevolution

22 **Introduction**

23 Biogeographical patterns in species richness are particularly well described and studied.
24 Identifying how eco-evolutionary processes shape species gradients is important for our basic
25 knowledge of the products of evolution and societal wellbeing, but an empirical understanding of
26 the processes causing these gradients has remained elusive (Etienne et al. 2019). Genetic
27 diversity is the most fundamental level of biodiversity. But until recently, comparable multi-
28 species, continent-wide data describing genome-wide variation was not available. These two
29 levels of diversity are so entangled that they are nearly inseparable. By not incorporating genetic
30 diversity into analyses of species richness we have been missing a critical piece of the complete
31 picture.

32

33 **Species richness gradients**

34 Relationships between species richness and environments suggest how we can integrate genetic
35 diversity into a joint analysis of both levels of variation. Though described as the latitudinal
36 species gradient, latitude can only be a correlate of the gradient's causes. Indeed, species
37 richness patterns sometimes deviate significantly from latitudinal trends, and these deviations
38 suggest its underlying causes. In North America (Simpson 1964) (Fig. 1) the latitudinal trend is
39 pronounced between the Arctic and the Canada-USA border (~50°N), before disappearing across
40 the continental USA and reappearing near its border with Mexico (~30°N). Species richness in
41 the continental USA varies longitudinally, peaking in the west. These deviations suggest that
42 species richness is correlated with environmental energy availability and habitat heterogeneity
43 (Simpson 1964; Kerr and Packer 1997), which in turn are both correlated with latitude in some
44 areas.

45 This pattern suggests that environments play a prominent role in determining species richness
46 and genetic diversity in at least two important ways. First, energy availability can impose an
47 upper limit on both the number of individuals and the number of species a given area can support
48 (the more-individuals hypothesis) (Storch et al. 2018). Diversity tends to increase with the
49 number of individuals in an assemblage, both in terms of the number of species in a community
50 (Hubbell 2001), and genetic diversity within populations (Kimura 1983). Second, more complex
51 environments have more niches. This can limit dispersal and support a greater diversity of
52 species, albeit at smaller population sizes, if those species come to specialize on different
53 resources (heterogeneity hypotheses) (Kadmon and Allouche 2007). As specialized populations
54 diverge, genetic variation will be divided among species that no longer interbreed. These smaller
55 populations will also lose genetic diversity due to genetic drift faster than large populations.

56

57 These two processes suggest that spatial variation at species and genetic levels are partly set by
58 environmental carrying capacities that limit the number of individuals and species a given area
59 can support. The effects of limited carrying capacity on genetic diversity at the population level
60 are well understood: smaller populations should be less diverse than larger populations due to
61 drift. Recent modelling suggests that carrying capacity, relative to other processes that also
62 produce gradients, is the strongest and most stable contributor to species richness (Etienne et al.
63 2019; Brodie 2019).

64

65 **Shared spatial variation in species and nuclear genetic gradients**

66 To test for shared spatial variation we quantified spatial patterns of nuclear genetic diversity for
67 North American mammals at a continental scale: the scale at which biogeographical diversity
68 patterns occur. To do this, we repurposed raw microsatellite genotypes posted in public data

69 repositories (Schmidt et al. 2020b). Microsatellite markers estimate genome-wide diversity—the
70 quantity we are interested in—well (Mittell et al. 2015). They were also the most commonly
71 archived marker type, which allowed us to maximize sample size. Our final data set consisted of
72 34,841 raw genotypes from 38 mammalian species sampled across 801 sites. We calculated gene
73 diversity, an estimate of the evenness and spread of alleles that is not particularly sensitive to
74 sample size (Fig. S1), for each site as our measure of genetic diversity (Charlesworth and
75 Charlesworth 2010). We then estimated species richness at each site by counting the number of
76 native mammal species whose ranges overlapped the site (IUCN 2019) so that we had directly
77 comparable estimates of diversity at the genetic and species levels. We summarized spatial
78 patterns in genetic diversity and species richness using distance-based Moran’s eigenvector maps
79 (MEMs) (Dray et al. 2006). Sixty-five percent of the variation in species richness and 24% of
80 variation in genetic diversity was spatial (Fig. S2). Variance partitioning suggested that 85% of
81 the total spatial variation in genetic diversity, and 32% of spatial variation in species richness
82 was accounted for by spatial patterns shared at both levels of diversity.

83
84 We used the linear regression predicted values of spatial vectors (MEMs), calculated above, that
85 had Moran’s I measures of spatial autocorrelation > 0.25 (indicating broad spatial patterns) to
86 produce maps of continental-scale spatial variation in both levels of diversity (Fig. 1). Consistent
87 with previously described patterns of species richness in North America, species richness
88 hotspots at our genetic sample sites appear to be related to topography, a measure of
89 environmental heterogeneity, and potential evapotranspiration, a measure of energy availability
90 (Fig. 1). There was no obvious relationship between latitude and nuclear genetic diversity.
91 Similar to patterns of species richness, a longitudinal gradient in genetic diversity is the
92 dominant pattern for North American mammals—however, diversity gradients at the two levels

93 trend in opposite richness. Genome-wide genetic diversity appears markedly lower in regions
94 with high species richness, such as on the west and mid-Atlantic coasts, where there is high
95 energy availability and topographic relief. This pattern is consistent with the prediction that these
96 areas would support more species with smaller, less genetically diverse populations. Our map of
97 neutral nuclear genetic diversity contrasts with relatively consistent latitudinal gradients in
98 mitochondrial (mtDNA) genetic diversity, the only other genetic marker explored at a similar
99 spatial scale (Miraldo et al. 2016; Theodoridis et al. 2020). This is perhaps not surprising because
100 mtDNA diversity is not systematically related to population size (Bazin et al. 2006), species
101 ecology, or life history (Nabholz et al. 2008)—all key features of the processes we explore here.

102

103 **Common causes of species and nuclear genetic gradients**

104 To explore the common causes of genetic and species-level diversity, we built a conceptual
105 model based on the idea that carrying capacity is a strong driver of diversity. We fit this
106 conceptual model to data using structural equation modelling, an approach for examining cause-
107 effect relationships within hypothesis networks that can accommodate multiple predictor and
108 response variables. Structural equation modelling is an extension of multivariate multiple
109 regression where variables can be thought of as nodes in a network, and directional paths
110 connecting nodes represent causal relationships. The strengths of paths are equal to regression
111 coefficients (Shipley 2016). In addition to direct effects, you can quantify indirect effects
112 between variables by multiplying direct effects over paths. Using standardized coefficients, we
113 can compare the strength of relationships both within and across levels of biodiversity. The
114 appropriateness of links in the hypothesis network can be tested using tests of directed separation
115 (Shipley 2016), where the null hypothesis is that the two variables are independent, conditional

116 on other predictors of either variable. This means that although we start with a focus on carrying
117 capacity, the data can suggest the addition or removal of links representing alternative
118 hypotheses.

119

120 Our conceptual model was built around the predicted effects of carrying capacity related to the
121 more individuals and environmental heterogeneity hypotheses (Fig 3a). The more individuals
122 hypothesis predicts that increasing energy availability should act through population size to
123 increase both species and genetic diversity. We use body size, which is inversely related to
124 population size, as our estimate of species-level population size (Damuth 1981). We measured
125 energy availability as the mean annual potential evapotranspiration across a species range.

126 Heterogeneity, measured at the range level by quantifying the area-corrected range in elevation
127 across a species range, should reduce population sizes but lead to greater species richness by
128 increasing niche diversity. Heterogeneity and energy availability were measured at the range-
129 level because the spatial coverage of genetic sample sites in the data is not evenly distributed.

130 Additionally, some species ranges could be oversampled if we considered population-level
131 environmental variation and thus overrepresented compared to species ranges that contain fewer
132 sampled populations. Finally, we included human population density in our model, predicting
133 negative relationships with species richness, genetic diversity, and mass (Merckx et al. 2018).
134 Contemporary rapid environmental change is rarely considered at the same time as long-term
135 processes, but humans are known to influence both levels of biodiversity and so should be
136 modelled.

137

138 Our final model fit the data well (SEM $p=0.23$, Fisher's $C=2.92$; Fig. 3b, Table S1). Energy
139 availability, niche heterogeneity, and human population density, acting both directly and

140 indirectly through species population size, explained 32% of the variation in genetic diversity.
141 The species-level variation explained by the random effect for species brought the total variation
142 in genetic diversity explained by our model to 75%. The same model explained 90% of the
143 variation in species richness. There was no strong spatial autocorrelation in the model,
144 suggesting that the spatial structure of the diversity data was well captured by our model
145 covariates (Fig. S3).

146
147 All links in our conceptual model were supported, with additional direct links suggested from
148 energy availability to species richness, genetic diversity to species richness, and heterogeneity to
149 genetic diversity (Fig 3b). Mammals conformed to the zero-sum carrying capacity related
150 expectations of the more individuals hypothesis at both genetic and species levels of biodiversity.
151 Our data indicated that when resources are limited, environmental carrying capacity is limited.
152 These environments supported fewer but larger-bodied species with smaller population sizes and
153 lower genetic diversity. In resource-rich areas, organisms are generally smaller, and populations
154 and communities larger, harboring greater genetic diversity and species richness. The strength of
155 effects related to the more individuals hypothesis was most prominent at the genetic level of
156 diversity: the strength of the indirect effect of energy on genetic diversity acting via population
157 size was 0.13 compared to 0.02 for species richness. We also detected a direct effect of energy
158 on species richness (path coefficient = 0.44 ± 0.01 SE; Fig. 3b, Table S1), even after accounting
159 for population size and topographic heterogeneity. This relationship has been noted elsewhere
160 and has sometimes been interpreted as refuting the more individuals hypothesis (Storch et al.
161 2018). Vegetation structure may drive the link between species richness and temperature
162 (Pautasso and Gaston 2005; Jiménez-Alfaro et al. 2016), as complex, vegetation-rich habitats in
163 warmer environments also have greater niche availability. Because both links are retained in our

164 model it seems clear that this additional link does not negate the more individuals hypothesis, but
165 rather is additive and indeed more important in determining species richness than the more
166 individuals effect.

167

168 Heterogeneity was the strongest single predictor of species richness (path coefficient = $0.70 \pm$
169 0.01), and a good predictor of genetic diversity (path coefficient = -0.30 ± 0.07). Directions of
170 effects were as expected if niche diversity reduces population sizes, carving existing variation
171 into multiple species and leading to increased drift (Fig. 2). Because gene diversity is not a
172 measure of divergence, we also tested whether environmental heterogeneity predicted
173 evolutionary divergence at the population level. To do this we calculated a population-specific
174 F_{ST} (Weir and Goudet 2017) from raw genotypes and related it to environmental heterogeneity.
175 Population-specific F_{ST} can be interpreted as a relative estimate of the time since a population
176 has diverged from a common ancestor. Results from this linear mixed model while controlling
177 for species as a random effect and spatial structure, showed that heterogeneity indeed increased
178 population divergence ($\beta = 0.13 \pm 0.06$ SE, $n = 785$ sites), suggesting that genetic drift is strong
179 and gene flow limited in these areas. Heterogeneous environments impose greater spatially
180 varying selection and coupled with low gene flow this creates ideal conditions for local
181 adaptation, which can happen even under relatively high levels of genetic drift (Hämälä et al.
182 2018). This lends support to the idea that there are higher diversification rates in more complex
183 environments because there are more opportunities for speciation.

184

185 Recent human-caused environmental disturbance both directly and indirectly (via body
186 mass/population size) affected both species and genetic diversity (Fig. 2b). Notably, although it
187 seems human presence and heterogeneity both reduce genetic diversity and limit dispersal,

188 human-dominated environments do not yet appear to be creating opportunities for coexistence by
189 niche-packing. Perhaps this will change with time, but if conditions for energetic requirements
190 and niche variability are not met, such a scenario is unlikely. Although a subset of species do
191 well in cities, the broader effects of habitat loss and homogenization make cities, as they are
192 currently built, inhospitable substitutes for the variety of natural niches they replace.

193

194 **Discussion**

195 The latitudinal species richness gradient has been recognized since the 1800s (Willig et al. 2003).
196 The gradient's consistency has generated >30 hypotheses aiming at explaining its relationship
197 with environments (Pontarp et al. 2019). Hypotheses fall into three broad categories:
198 evolutionary time, diversification rates, and ecological limits (differential carrying capacities),
199 which are often, at least implicitly, treated as competing ideas. But we cannot have speciation
200 without ecology and evolution. Pontarp and Wiens (2017) advocate a more interconnected view,
201 reporting that time for speciation effects on diversity should be strongest at short time scales,
202 especially during the initial colonization of new environments. When all locales are colonized,
203 habitats that provide more opportunities for speciation should over time become the most
204 diverse. All the while, differential carrying capacities determine demographic parameters such as
205 colonization success, population viability, and risk of local extinction, as well as the efficiency of
206 selection. Etienne et al. (2019) used simulations to determine that ecological limits on carrying
207 capacity present the most parsimonious explanation for the latitudinal diversity gradient, though
208 all categories of hypothesis produced gradients. Worm and Tittensor (2018) were able to recreate
209 diversity gradients with simulations using only two parameters: temperature and community size.
210 Also using simulations, Vellend (2005) found that by increasing environmental heterogeneity,

211 rare species increased in abundance so much that the population size and genetic diversity of
212 other species in the community decreased. Our findings, explaining 75 and 90% of the variation
213 in genetic diversity and species richness respectively, provide strong empirical support for the
214 theory-based inferences described above and extend them to the genetic level—multiple eco-
215 evolutionary processes simultaneously produce the gradients in genetic and species level
216 biodiversity we see in nature.

217

218 Communities with diverse species provide important ecosystem functions and services that
219 contribute to human physical and psychological well-being. Ecosystem sustainability in the face
220 of environmental perturbations, occurring more frequently due to human causes, depends on the
221 resiliency of landscapes, communities, and populations (Oliver et al. 2015). The intimate
222 connections between the environment, species richness and genetic diversity we find here
223 suggest that changes on one level can cascade throughout the system and profoundly reshape
224 broad patterns of global biodiversity across multiple biological levels in ways we do not yet fully
225 grasp. Tradeoffs between genetic and species level biodiversity present a conundrum for
226 management practitioners because complex environments that are hotspots for species richness
227 are more likely to harbor relatively low intraspecific genetic variation, and consequently
228 populations that may be less resilient to environmental change. Thus it appears designating
229 conservation areas with the preservation of both species and genetic diversity in mind is not an
230 advisable strategy. Instead, programs focusing on conserving environments and native biological
231 communities should be separate from those aiming to preserve population size and standing
232 genetic variation.

233

234 **Acknowledgements:** We would like to thank the Population Ecology and Evolutionary Genetics
235 group for their feedback on this manuscript. We are also grateful to the authors whose work
236 provided the raw data for this synthesis. C.S. and C.J.G. were supported by a Natural Sciences
237 and Engineering Research Council of Canada Discovery Grant to C.J.G. C.S. was also supported
238 by a U. Manitoba Graduate Fellowship, and a U. Manitoba Graduate Enhancement of Tri-council
239 funding grant to C.J.G.

240 **Author contributions:** C.J.G. and C.S. conceptualized the study. C.S., S.D. and C.J.G. designed
241 the study and C.S. conducted the statistical analysis with input from S.D. and C.J.G. All authors
242 contributed to data interpretation. C.S. wrote the first draft of the manuscript and all authors
243 participated in editing subsequent manuscript drafts.

244

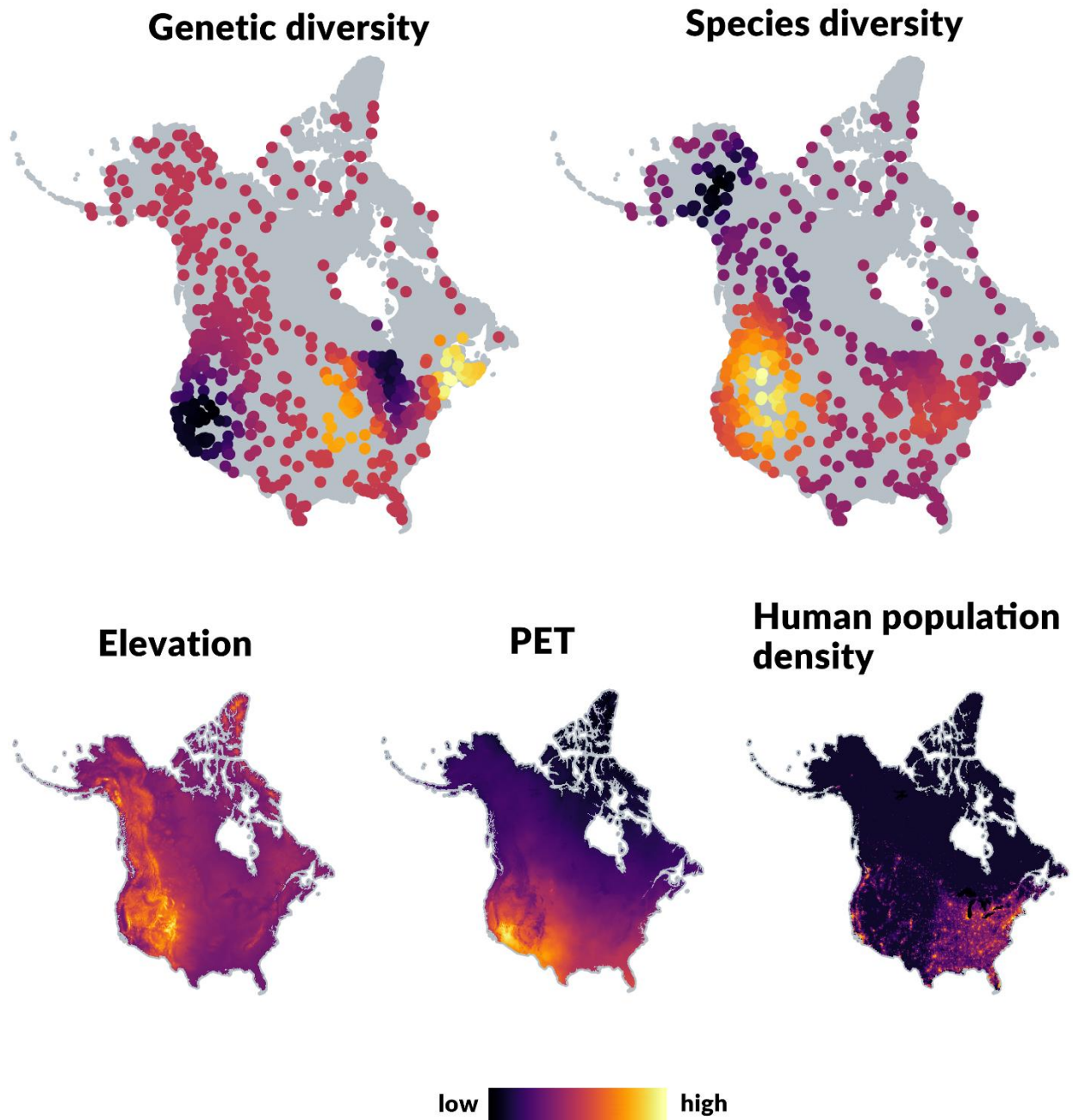
245 **References**

- 246 Bazin, E., Glémin, S., and Galtier, N. 2006. Population size does not influence mitochondrial
247 genetic diversity in animals. *Science*. **312**(5773): 570–572. doi:10.1126/science.1122033.
- 248 Blanchet, G.F., Legendre, P., and Borcard. 2008. Forward Selection of Explanatory Variables.
249 *Ecology* **89**(9): 2623–2632.
- 250 Borcard, D., and Legendre, P. 2002. All-scale spatial analysis of ecological data by means of
251 principal coordinates of neighbour matrices. *Ecol. Modell.* **153**(1–2): 51–68.
252 doi:10.1016/S0304-3800(01)00501-4.
- 253 Borcard, D., Legendre, P., Avois-Jacquet, C., and Tuomisto, H. 2004. Dissecting the Spatial
254 Structure of Ecological Data at Multiple Scales. *Ecology* **85**(7): 1826–1832.
- 255 Brodie, J.F. 2019. Environmental limits to mammal diversity vary with latitude and global
256 temperature. *Ecol. Lett.* **22**(3): 480–485. doi:10.1111/ele.13206.
- 257 Charlesworth, B., and Charlesworth, D. 2010. *Elements of Evolutionary Genetics*. Roberts &
258 Company Publishers, Greenwood Village, Colorado, USA.
- 259 Currie, D.J. 1991. Energy and Large-Scale Patterns of Animal- and Plant-Species Richness. *Am.*
260 *Nat.* **137**(1): 27–49.
- 261 Damuth, J. 1981. Population density and body size in mammals. *Nature* **290**(April): 1980–1981.

- 262 Dray, S., Legendre, P., and Peres-Neto, P.R. 2006. Spatial modelling: a comprehensive
263 framework for principal coordinate analysis of neighbour matrices (PCNM). *Ecol. Modell.*
264 **196**(3–4): 483–493. doi:10.1016/j.ecolmodel.2006.02.015.
- 265 Etienne, R.S., Cabral, J.S., Hagen, O., Hartig, F., Hurlbert, A.H., Pellissier, L., Pontarp, M., and
266 Storch, D. 2019. A Minimal Model for the Latitudinal Diversity Gradient Suggests a
267 Dominant Role for Ecological Limits. *Am. Nat.* **194**(5): E000–E000. doi:10.1086/705243.
- 268 Fisher, J.B., Whittaker, R.J., and Malhi, Y. 2011. ET come home: Potential evapotranspiration in
269 geographical ecology. *Glob. Ecol. Biogeogr.* **20**(1): 1–18. doi:10.1111/j.1466-
270 8238.2010.00578.x.
- 271 Hämälä, T., Mattila, T.M., and Savolainen, O. 2018. Local adaptation and ecological
272 differentiation under selection, migration and drift in *Arabidopsis lyrata*. *Evolution.*
273 doi:10.1111/evo.13502.
- 274 Hubbell, S.P. 2001. *The Unified Neutral Theory of Biodiversity and Biogeography*. Princeton
275 University Press, Princeton NJ.
- 276 IUCN. 2019. *The IUCN Red List of Threatened Species*. Version 2019-1. Available from
277 <https://www.iucnredlist.org>.
- 278 Jiménez-Alfaro, B., Chytrý, M., Mucina, L., Grace, J.B., and Rejmánek, M. 2016. Disentangling
279 vegetation diversity from climate-energy and habitat heterogeneity for explaining animal
280 geographic patterns. *Ecol. Evol.* **6**(5): 1515–1526. doi:10.1002/ece3.1972.
- 281 Jones, K.E., Bielby, J., Cardillo, M., Fritz, S.A., O’Dell, J., Orme, C.D.L., Safi, K., Sechrest, W.,
282 Boakes, E.H., Carbone, C., Connolly, C., Cutts, M.J., Foster, J.K., Grenyer, R., Habib, M.,
283 Plaster, C.A., Price, S.A., Rigby, E.A., Rist, J., Teacher, A., Bininda-Emonds, O.R.P.,
284 Gittleman, J.L., Mace, G.M., and Purvis, A. 2009. PanTHERIA: a species-level database of
285 life history, ecology, and geography of extant and recently extinct mammals. *Ecology*
286 **90**(9): 2648–2648. doi:10.1890/08-1494.1.
- 287 Kadmon, R., and Allouche, O. 2007. Integrating the effects of area, isolation, and habitat
288 heterogeneity on species diversity: A unification of island biogeography and niche theory.
289 *Am. Nat.* **170**(3): 443–454. doi:10.1086/519853.
- 290 Kerr, J.T., and Packer, L. 1997. Habitat heterogeneity as a determinant of mammal species
291 richness. *Nature* **385**: 253–254.
- 292 Kimura, M. 1983. *The Neutral Theory of Molecular Evolution*. Cambridge University Press,
293 Cambridge.
- 294 Kreft, H., and Jetz, W. 2007. Global patterns and determinants of vascular plant diversity. *Proc.*
295 *Natl. Acad. Sci.* **104**(14): 5925–5930. doi:10.1073/pnas.0608361104.
- 296 Lefcheck, J., Byrnes, J., and Grace, J. 2019. piecewiseSEM: Piecewise Structural Equation
297 Modeling. Available from <https://cran.r-project.org/package=piecewiseSEM>.
- 298 Lefcheck, J.S. 2016. piecewiseSEM: Piecewise structural equation modelling in r for ecology,
299 evolution, and systematics. *Methods Ecol. Evol.* **7**(5): 573–579. doi:10.1111/2041-
300 210X.12512.

- 301 Manel, S., Gugerli, F., Thuiller, W., Alvarez, N., Legendre, P., Holderegger, R., Gielly, L., and
302 Taberlet, P. 2012. Broad-scale adaptive genetic variation in alpine plants is driven by
303 temperature and precipitation. *Mol. Ecol.* **21**(15): 3729–3738. doi:10.1111/j.1365-
304 294x.2012.05656.x.
- 305 Merckx, T., Souffreau, C., Kaiser, A., Baardsen, L.F., Backeljau, T., Bonte, D., Brans, K.I.,
306 Cours, M., Dahirel, M., Debortoli, N., De Wolf, K., Engelen, J.M.T., Fontaneto, D.,
307 Gianuca, A.T., Govaert, L., Hendrickx, F., Higuity, J., Lens, L., Martens, K., Matheve, H.,
308 Matthysen, E., Piano, E., Sablon, R., Schön, I., Van Doninck, K., De Meester, L., and Van
309 Dyck, H. 2018. Body-size shifts in aquatic and terrestrial urban communities. *Nature*
310 **558**(7708): 113–116. doi:10.1038/s41586-018-0140-0.
- 311 Miraldo, A., Li, S., Borregaard, M.K., Florez-Rodriguez, A., Gopalakrishnan, S., Rizvanovic,
312 M., Wang, Z., Rahbek, C., Marske, K.A., and Nogues-Bravo, D. 2016. An Anthropocene
313 map of genetic diversity. *Science.* **353**(6307): 1532–1535. doi:10.1126/science.aaf4381.
- 314 Mittell, E.A., Nakagawa, S., and Hadfield, J.D. 2015. Are molecular markers useful predictors of
315 adaptive potential? *Ecol. Lett.* **18**(8): 772–778. doi:10.1111/ele.12454.
- 316 Nabholz, B., Mauffrey, J.F., Bazin, E., Galtier, N., and Glemin, S. 2008. Determination of
317 mitochondrial genetic diversity in mammals. *Genetics* **178**(1): 351–361.
318 doi:10.1534/genetics.107.073346.
- 319 NOAA, and U.S. National Geophysical Data Center. (n.d.). TerrainBase, release 1.0. Boulder
320 CO. Available from [https://nelson.wisc.edu/sage/data-and-](https://nelson.wisc.edu/sage/data-and-models/atlas/maps.php?datasetid=28&includerelatedlinks=1&dataset=28)
321 [models/atlas/maps.php?datasetid=28&includerelatedlinks=1&dataset=28](https://nelson.wisc.edu/sage/data-and-models/atlas/maps.php?datasetid=28&includerelatedlinks=1&dataset=28).
- 322 Oliver, T.H., Heard, M.S., Isaac, N.J.B., Roy, D.B., Procter, D., Eigenbrod, F., Freckleton, R.,
323 Hector, A., Orme, C.D.L., Petchey, O.L., Proença, V., Raffaelli, D., Suttle, K.B., Mace,
324 G.M., Martín-López, B., Woodcock, B.A., and Bullock, J.M. 2015. Biodiversity and
325 Resilience of Ecosystem Functions. *Trends Ecol. Evol.* **30**(11): 673–684. Elsevier Ltd.
326 doi:10.1016/j.tree.2015.08.009.
- 327 Pautasso, M., and Gaston, K.J. 2005. Resources and global avian assemblage structure in forests.
328 *Ecol. Lett.* **8**(3): 282–289. doi:10.1111/j.1461-0248.2005.00724.x.
- 329 Pontarp, M., Bunnefeld, L., Cabral, J.S., Etienne, R.S., Fritz, S.A., Gillespie, R., Graham, C.H.,
330 Hagen, O., Hartig, F., Huang, S., Jansson, R., Maliet, O., Münkemüller, T., Pellissier, L.,
331 Rangel, T.F., Storch, D., Wiegand, T., and Hurlbert, A.H. 2019. The Latitudinal Diversity
332 Gradient: Novel Understanding through Mechanistic Eco-evolutionary Models. *Trends*
333 *Ecol. Evol.*: 1–13. doi:10.1016/j.tree.2018.11.009.
- 334 Pontarp, M., and Wiens, J.J. 2017. The origin of species richness patterns along environmental
335 gradients: uniting explanations based on time, diversification rate and carrying capacity. *J.*
336 *Biogeogr.* **44**(4): 722–735. doi:10.1111/jbi.12896.
- 337 R Core Team. 2013. R: A Language and Environment for Statistical Computing. Vienna,
338 Austria. Available from <http://www.r-project.org/>.
- 339 Schmidt, C., Domaratzki, M., Kinnunen, R.P., Bowman, J., and Garroway, C.J. 2020a. Data
340 from: Continent-wide effects of urbanization on bird and mammal genetic diversity. Dryad

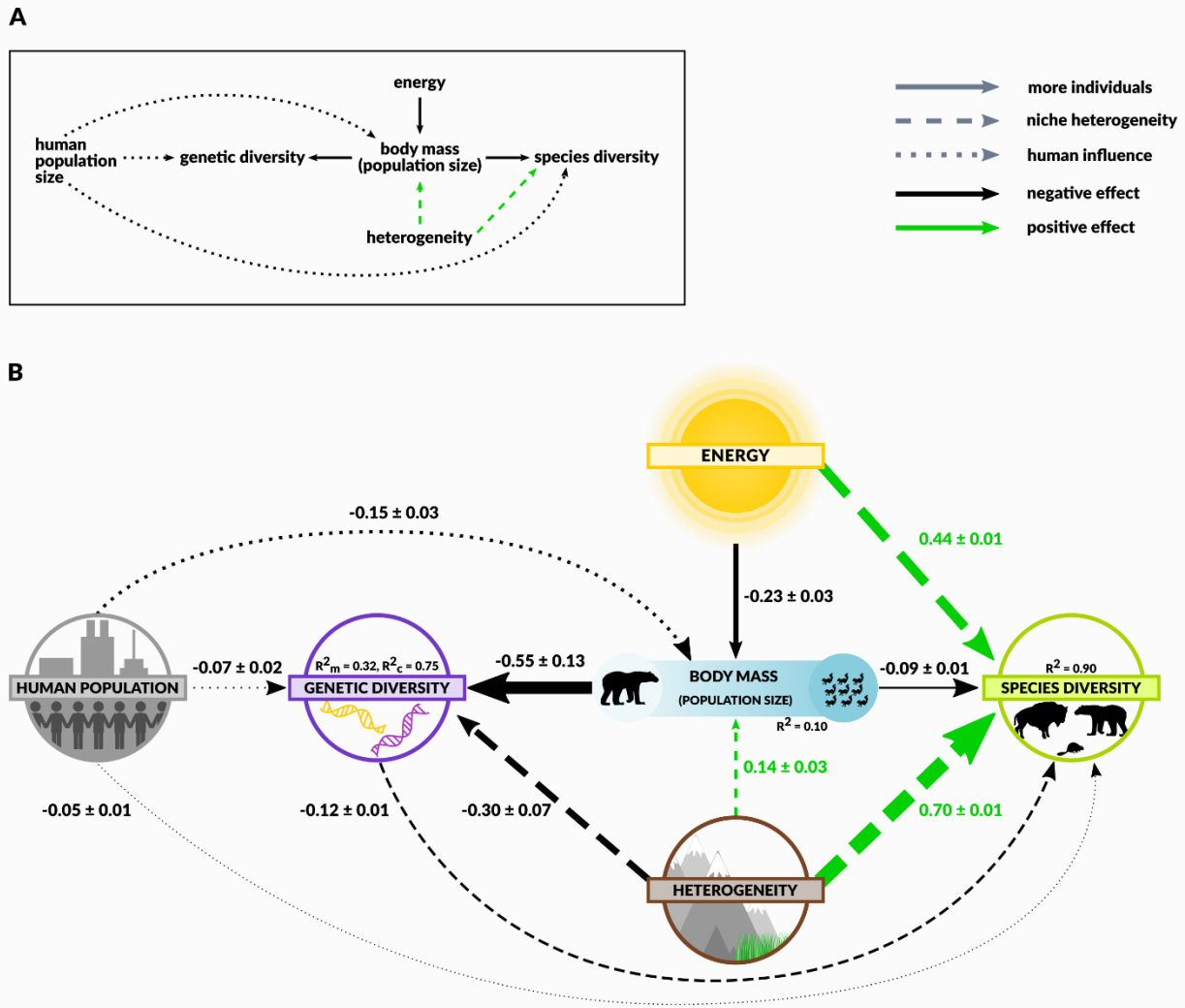
- 341 Data Repository. doi:10.5061/dryad.cz8w9gj0c.
- 342 Schmidt, C., Domaratzki, M., Kinnunen, R.P., Bowman, J., and Garroway, C.J. 2020b.
343 Continent-wide effects of urbanization on bird and mammal genetic diversity. *Proc. R. Soc.*
344 *B Biol. Sci.* **287**(1920): 20192497. doi:10.1098/rspb.2019.2497.
- 345 Shipley, B. 2016. Cause and Correlation in Biology. *In* Cause and Correlation in Biology, 2nd
346 edition. Cambridge University Press, Cambridge.
- 347 Simpson, G.G. 1964. Species Density of North American Recent Mammals. *Syst. Zool.* **13**(2):
348 57–73.
- 349 Storch, D., Bohdalková, E., and Okie, J. 2018. The more-individuals hypothesis revisited: the
350 role of community abundance in species richness regulation and the productivity–diversity
351 relationship. *Ecol. Lett.* **21**(6): 920–937. doi:10.1111/ele.12941.
- 352 Theodoridis, S., Fordham, D.A., Nogues-bravo, D., and Brown, S.C. 2020. Evolutionary history
353 and past climate change shape the distribution of genetic diversity in terrestrial mammals.
354 *Nat. Commun.*: 1–11. Springer US. doi:10.1038/s41467-020-16449-5.
- 355 Trabucco, A., and Zomer, R. 2019. Global Aridity Index and Potential Evapotranspiration (ET0)
356 Climate Database v2. doi:10.6084/m9.figshare.7504448.v3.
- 357 Vellend, M. 2005. Species Diversity and Genetic Diversity: Parallel Processes and Correlated
358 Patterns. *Am. Nat.* **166**(2): 199–215. doi:10.1086/431318.
- 359 Weir, B.S., and Goudet, J. 2017. A Unified Characterization of Population Structure. *Genetics*
360 **206**: 2085–2103.
- 361 Willig, M.R., Kaufman, D.M., and Stevens, R.D. 2003. Latitudinal Gradients of Biodiversity:
362 Pattern, Process, Scale, and Synthesis. *Annu. Rev. Ecol. Evol. Syst.* **34**(1): 273–309.
363 doi:10.1146/annurev.ecolsys.34.012103.144032.
- 364 Worm, B., and Tittensor, D.P. 2018. A Theory of Global Biodiversity. Princeton University
365 Press, Princeton, New Jersey.



366

367

368 **Fig. 1.** Maps depicting spatial patterns of biodiversity and environmental factors. (*Top row*)
369 Points are the locations of 801 North American mammal populations for which raw
370 microsatellite data was available in public repositories. Point color indicates predicted values of
371 genetic diversity and species richness based on spatial patterns detected in the data. (*Bottom row*)
372 Maps showing the three environmental variables which we tested for simultaneous effects on
373 genetic diversity and species richness.



374
375
376
377
378
379
380
381
382
383
384
385

Fig. 2. (a) Our conceptual hypothesis network combining the more individuals hypothesis (solid lines) with the effects of environmental heterogeneity (dashed lines) and human presence (dotted lines). Arrows represent unidirectional relationships between variables. (b) Structural equation model results. Green and black lines positive and negative relationships, respectively. Line widths reflect coefficient estimates, which are listed above each path with standard errors. R^2 values are the amount of variation explained for each response variable. Mass and species richness were measured at the species level, and genetic diversity was measured at the population level and fit with a random effect for species: R^2_m is the variation explained by fixed effects only, and R^2_c is the variation explained by fixed and random effects.

386 **Supplementary Information**

387 **Methods**

388 Data assembly

389 *Genetic diversity and body size.* We obtained estimates of neutral genetic diversity at 801 sites
390 across North America from the database compiled by Schmidt et al. (Schmidt et al. 2020a,
391 2020b), where diversity metrics for each site were computed from raw georeferenced
392 microsatellite data . We chose gene diversity at each site as our metric for genetic diversity. Gene
393 diversity estimates the richness and evenness of alleles in a population and is minimally affected
394 by sample size (Charlesworth and Charlesworth 2010). Next, we recorded mean adult body mass
395 (g) for each species using data from the PanTHERIA database (Jones et al. 2009). Mass was log-
396 transformed in our models.

397 *Species richness.* We downloaded range maps for terrestrial mammals native to North America
398 from the IUCN Red List database (IUCN 2019). Ranges for all species were mapped in a single
399 Esri shapefile layer with polygon features. We filtered these maps to retain ranges for extant,
400 native, resident, mainland species in ArcMap Desktop 10.3.1 (ESRI, Redlands, CA). We
401 estimated species richness at each of our genetic diversity sample sites to describe spatial
402 variation at both levels of biodiversity across North America. We used a spatial join to count the
403 number of species ranges which overlapped each site to provide a site-level index of species
404 richness. For a broader scale measure of species richness, we also measured richness at the level
405 of each species' range. We did this to avoid introducing bias in biodiversity patterns at the
406 continental scale due to the spread of our genetic diversity sites, which did not consistently
407 sample a species' entire range. We computed species-level species richness by counting the

408 number of intersecting species ranges using a spatial join in ArcMap. To correct for potential
409 biases due to differences in range size, we divided the number of overlapping ranges by the
410 species' range area (km²).

411 *Environmental variables.* Potential evapotranspiration measures the atmosphere's ability to
412 remove water from the Earth's surface, and is an indicator of atmospheric energy availability.
413 Potential evapotranspiration is one of the strongest environmental correlates of species richness
414 in mammals (Currie 1991; Kreft and Jetz 2007; Fisher et al. 2011; Jiménez-Alfaro et al. 2016).
415 We estimated mean potential evapotranspiration (mm/yr) within each species' range using
416 annual potential evapotranspiration data from 1970-2000 available via the CGIAR Consortium
417 for Spatial Information (Trabucco and Zomer 2019). We used a global topography map (NOAA
418 and U.S. National Geophysical Data Center) to record the range in elevation across focal species
419 ranges to quantify environmental heterogeneity. We also corrected elevation range for potential
420 biases introduced by species range area, because larger ranges tended to encompass greater
421 topographical heterogeneity. Human population sizes were recorded for each site in the
422 aforementioned genetic diversity database (Schmidt et al. 2020a).

423 Analysis

424 *Spatial patterns in genetic diversity and species richness.* All analyses were conducted in R
425 (version 3.6.1, R Core Team 2013). Our first step was to identify spatial patterns in genetic
426 diversity. We accomplished this by adopting a method used in landscape genetics to control for
427 unmeasured environmental variables when investigating adaptive variation associated with
428 environmental factors (Manel et al. 2012). Distance-based Moran's eigenvector maps (MEMs)
429 detect spatial patterns in data from a modified matrix of distances between sites—a 'neighbor'

430 matrix—whose eigenvalues are proportional to Moran’s I index of spatial autocorrelation
431 (Borcard and Legendre 2002; Borcard et al. 2004; Dray et al. 2006). MEMs are vectors that
432 represent spatial relationships between sites at all scales detectable by the sampling scheme, and
433 can be included in linear models to account for effects of unknown spatial processes. Our next
434 step was to determine which MEMs reflected important spatial patterns in genetic diversity and
435 site-level species richness, using a forward selection procedure (Blanchet et al. 2008). This gave
436 us two sets of MEMs which described spatial patterns present in genetic diversity and species
437 richness. To produce continental maps of genetic and species levels of biodiversity we selected
438 MEMs which modeled broad scale spatial patterns based on Moran’s I (MEMs with Moran’s I >
439 0.25). We then fit individual linear regression models for species and genetic diversity with
440 corresponding MEMs, and plotted the predicted values.

441 *Variation partitioning.* We then examined the extent to which genetic diversity and species
442 richness covary spatially. Because MEMs for species richness and genetic diversity were
443 computed from the same set of coordinates, they were directly comparable: this allowed us to
444 identify shared spatial patterns that might have a common environmental cause. We used linear
445 regressions and variance partitioning to determine what fraction of the total variation in species
446 richness and genetic diversity could be attributed to: (1) non-spatial variation, (2) non-shared
447 shared spatial variation, and (3) shared spatial variation.

448 *Joint analysis of causes of genetic diversity and species richness.* Next, we tested the hypothesis
449 that differential carrying capacities are important drivers of biodiversity, specifically the more
450 individuals hypothesis and the effects of environmental heterogeneity and human activity. We
451 developed a causal framework based on these hypotheses (Fig. 3a) which we tested using
452 structural equation modeling (SEM). SEM is an extension of multivariate regression in which a

453 series of regressions representing causal relationships between variables are assessed as
454 components of a hypothesis network (Shipley 2016). We implemented SEMs in the
455 piecewiseSEM package (Lefcheck 2016; Lefcheck et al. 2019). PiecewiseSEM offers greater
456 flexibility than other SEM software because it uses a local estimation approach where each
457 model is assessed individually (Lefcheck 2016). This frees the user from assuming multivariate
458 normality and linear relationships between variables when using global estimation to evaluate
459 SEM fit. All variables were scaled and centered prior to analysis.

460 We translated our conceptual diagram (Fig. 3a) into a network of 3 linear models with a single
461 model for each response variable: gene diversity, body size, and species richness. Gene diversity
462 was measured for populations nested within species, thus we used a hierarchical model within
463 the SEM framework to control for species differences by fitting it as a random effect.

464 Goodness-of-fit in SEM is determined by evaluating whether there are any missing links in the
465 causal structure, i.e. whether adding paths between pairs of variables would be more consistent
466 with the data. In piecewiseSEM missing links are tested using tests of directed separation
467 (Shipley 2016), where the null hypothesis is that the two variables are independent, conditional
468 on other predictors of either variable. Starting with our conceptual model (Fig. 3a), we iteratively
469 updated models by adding links according to tests of directed separation until no further
470 biologically sensible links were suggested. A non-sensible link, for example, would be genetic
471 diversity causing energy availability. We assessed model fit using the p -value for the model
472 network, where the null hypothesis is that the model is consistent with the data. Thus, models
473 with $p > 0.05$ are considered acceptable – we fail to reject our causal structure. We also assessed
474 fit using R^2 values for each response variable in the model network. For genetic diversity, we
475 used marginal (R^2_m) and conditional R^2 (R^2_c) values which respectively measure the total

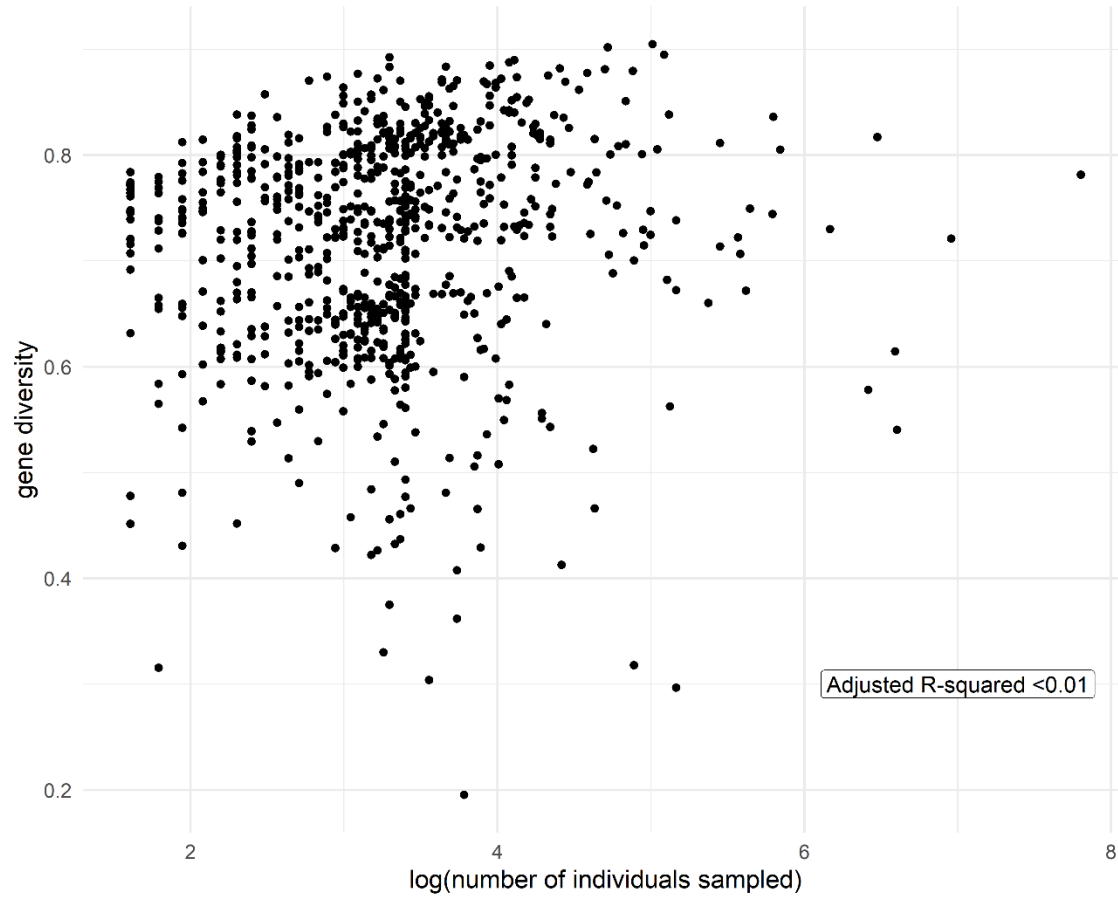
476 variation explained by fixed effects and the variation explained by both fixed and random
477 effects. We then tested the residuals from component models for spatial autocorrelation using
478 Moran's tests and spatial correlograms. The body size model residuals were not spatially
479 autocorrelated, but genetic diversity and species richness models had statistically significant
480 spatially autocorrelated residuals at very local scales (genetic diversity Moran's $I = 0.025$,
481 species richness Moran's $I = 0.029$). These Moran's I values do not indicate strong spatial
482 structure in the data and we decided not to integrate it into our model. The positive spatial
483 autocorrelation at such short distances is likely an artifact of irregular site locations and the
484 hierarchical nature of the data.

485 *Effect of heterogeneity on population divergence.* We tested whether topographic heterogeneity
486 caused greater population differentiation using population-specific F_{ST} (Weir and Goudet 2017),
487 a measure of genetic divergence. We controlled for isolation-by-distance by including dbMEMs
488 significantly related to F_{ST} to account for spatial structure. We scaled and centered all variables,
489 then used a linear mixed model of the form: $F_{ST} \sim heterogeneity + MEMs + (1/species)$,
490 controlling for species differences by including it as a random effect.

491 **Supplementary Results**

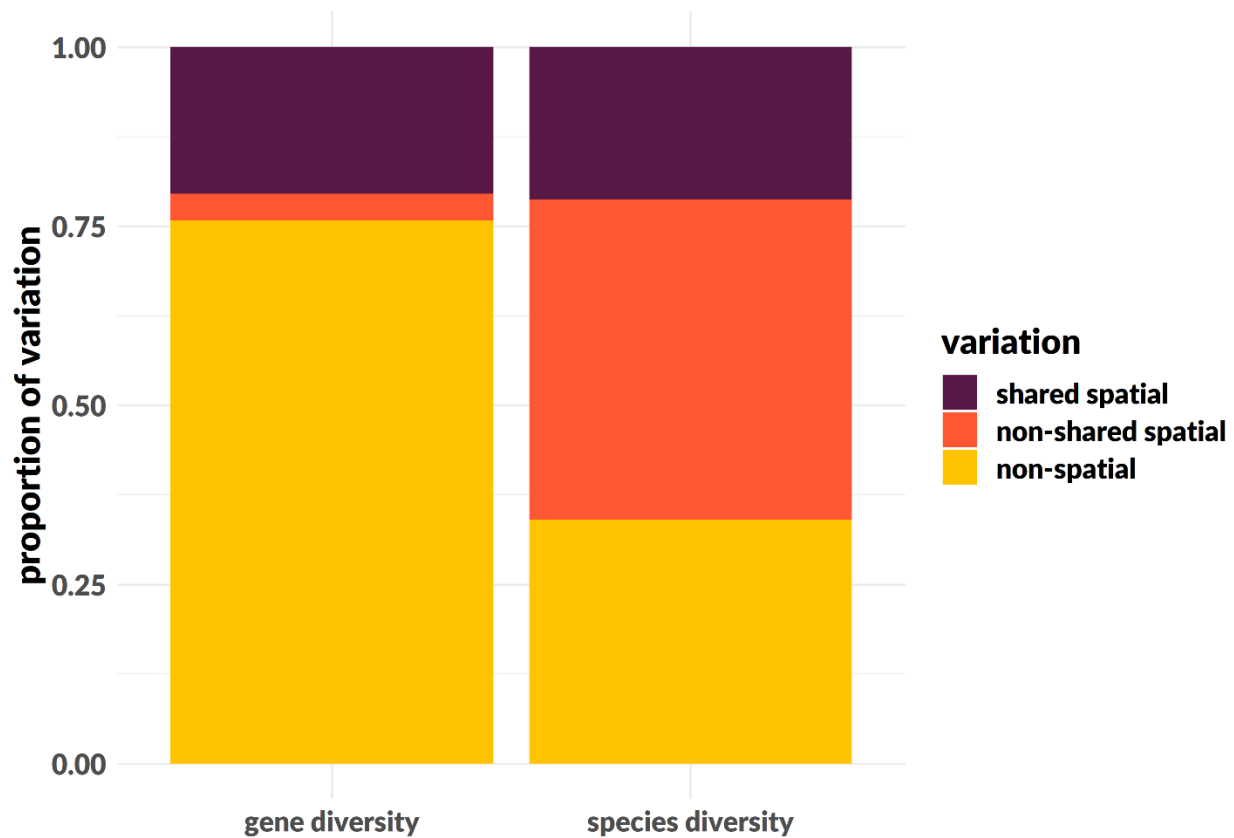
492 *Spatial patterns in genetic diversity and species richness.* We detected spatial patterns in genetic
493 diversity at several scales. A total of 199 MEMs corresponded to positive spatial autocorrelation.
494 Of these, 13 explained important spatial variation in gene diversity. In order of increasingly fine
495 spatial scales, significant patterns were MEMs 2, 3, 4, 5, 22, 27, 30, 31, 47, 49, 101, 145, 152.
496 Forty-three MEMs were important predictors of species richness, and 8 of these patterns were
497 shared by genetic diversity (Fig. S1). The cut-off for broad-scale MEMs—defined as those

498 having Moran's I values > 0.25 —was MEM 5 for genetic diversity and MEM 11 for species
499 richness.



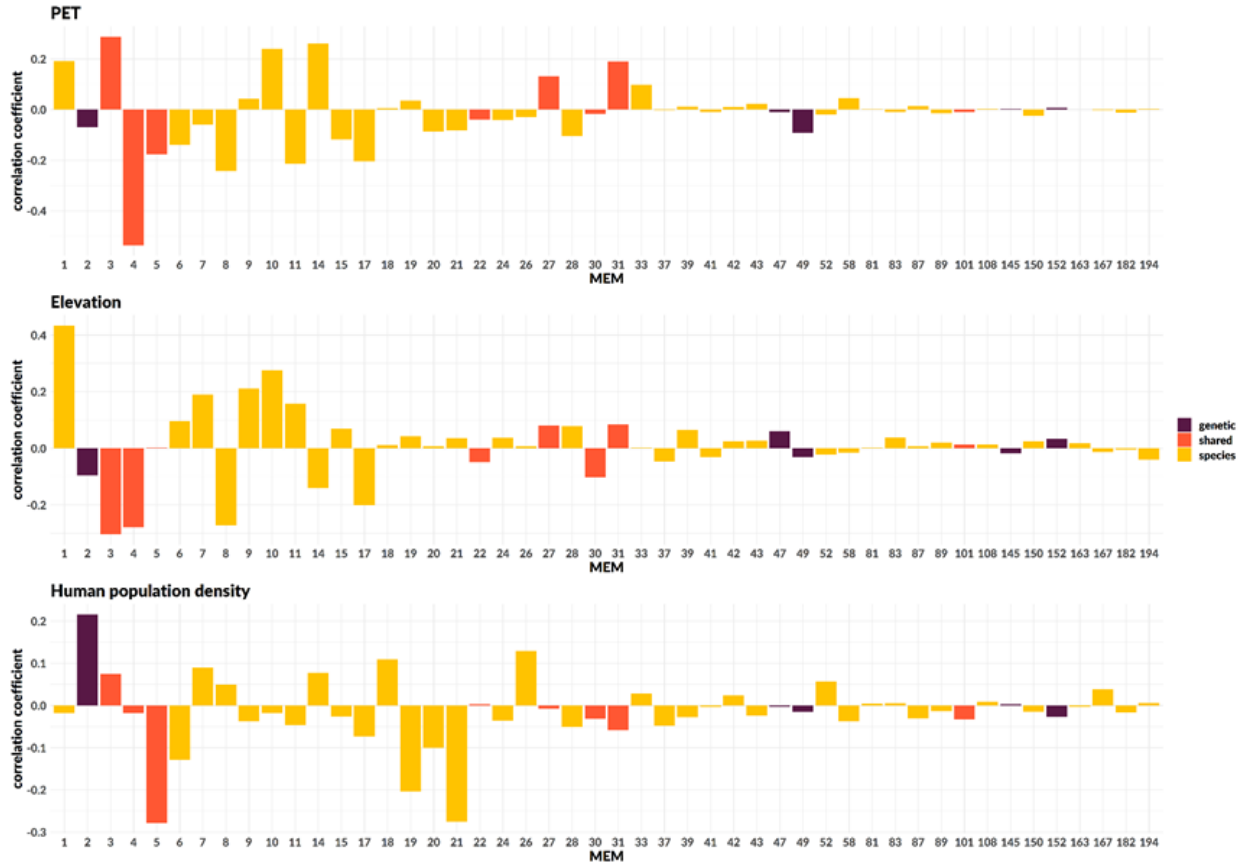
500

501 **Figure S1.** Plot of gene diversity vs. sample size. Gene diversity as a metric of genetic diversity
502 depends on allele frequencies and is minimally affected by sample size. Larger populations have
503 more rare alleles, which contribute little to gene diversity.



504
505
506
507
508
509
510

Fig. S2. Variation partitioning results. This graph shows the proportion of variation in genetic diversity and species richness which can be explained by spatial factors, determined using Moran's eigenvector maps (MEMs). Spatial variation is further broken down into shared and non-shared spatial variation. Shared spatial variation is variation in genetic diversity and species richness explained by shared MEMs; non-shared variation is the remaining fraction of spatial variation not accounted for by shared MEMs.



511

512 **Figure S3.** Correlation coefficients for spatial patterns (MEMs) and environmental variables
513 measured at the site level: potential evapotranspiration (PET), elevation, and human population
514 density. MEMs describe spatial patterns in genetic diversity, species richness, or both (shared
515 spatial patterns). MEMs are ordered from broad (MEM1) to fine scale (MEM194) patterns.
516 Strong correlations indicate that environmental variables included in structural equation models
517 account for broad scale spatial patterns present in genetic diversity and species richness.

518 **Table S1.** Path coefficients and standard errors for SEM model (Fisher's $C = 2.92$, $p = 0.23$, 2
519 degrees of freedom).

Response	Predictor	Estimate \pm SE
genetic diversity	human population density	-0.07 \pm 0.02
genetic diversity	mass	-0.55 \pm 0.13
genetic diversity	heterogeneity	-0.30 \pm 0.07
mass	PET	-0.23 \pm 0.03
mass	heterogeneity	0.14 \pm 0.03
mass	human population density	-0.15 \pm 0.03
species richness	mass	-0.09 \pm 0.01
species richness	heterogeneity	0.70 \pm 0.01
species richness	human population density	-0.05 \pm 0.01
species richness	PET	0.44 \pm 0.01
species richness	genetic diversity	-0.12 \pm 0.01

520